

Cite this article as:  
Thiravit S, Teerasamit W, Thiravit P. The different faces of renal angiomyolipomas on radiologic imaging: a pictorial review. *Br J Radiol* 2018; **91**: 20170533.

## PICTORIAL REVIEW

# The different faces of renal angiomyolipomas on radiologic imaging: a pictorial review

SHANIGARN THIRAVIT, MD, WANWARANG TEERASAMIT, MD and PHAKPHOOM THIRAVIT, MD

Department of Radiology, Faculty of Medicine Siriraj Hospital, Mahidol University, Bangkok, Thailand

Address correspondence to: Dr Shanigarn Thiravit  
E-mail: [thiravit.mahidol@gmail.com](mailto:thiravit.mahidol@gmail.com)

### ABSTRACT

Renal angiomyolipoma (AML) is an uncommon renal tumour, generally composed of mature adipose tissue, dysmorphic blood vessels and smooth muscle. Identification of intratumoral fat on unenhanced CT images is the most reliable finding for establishing the diagnosis of renal AML. However, AMLs sometimes exhibit atypical findings, including cystic as well as solid forms; some of these variants overlap with the appearance of other renal tumours. A rare type of AML, the epithelioid type, possesses malignant potential. The aim of this pictorial review is to gather the different imaging features of AMLs including the classic and fat-poor types, AMLs with epithelial cysts, epithelioid AML, AML associated with tuberous sclerosis, haemorrhagic AML and large AMLs mimicking retroperitoneal liposarcomas. The diagnostic clues that help to distinguish AMLs from other renal tumours are also described in the review.

### INTRODUCTION

Renal angiomyolipoma (AML) is an uncommon renal tumour, usually discovered incidentally on diagnostic imaging. Renal AMLs occur more in females than in males.<sup>1</sup> About 80% of renal AMLs are sporadic, usually occurring in the fifth decade. The other 20% are associated with tuberous sclerosis complex (TSC) and occur in a younger age group, usually the third decade.<sup>2</sup> AML is also associated with lymphangiomyomatosis.<sup>1</sup>

Once considered a benign renal hamartoma, renal AML has been recognized as part of the family of perivascular epithelioid cell tumours (PEComas), that express myogenic (human melanosome B [HMB]-45) and melanocytic (actin and/or desmin) markers.<sup>1</sup> The PEComas also relate to TSC due to losses of TSC1 or TSC2 genes that may have a role in the regulation of the mammalian target of rapamycin pathway.<sup>2</sup>

Renal AMLs are triphasic tumours, composed of mature adipose tissue, dysmorphic blood vessels, and smooth muscle in varying proportions, which contribute to the imaging characteristics. AMLs sometimes present with atypical findings and may mimic renal cell carcinoma (RCC). Recently, two radiologic classifications of renal AMLs have been introduced. Jinzaki et al categorized them into classic and fat-poor subtypes, and another classification by Song et al categorized them into fat-rich, fat-poor,

and fat-invisible subtypes.<sup>1,3</sup> In this pictorial review, CT and MRI features of classic and fat-poor AMLs, AMLs with epithelial cysts (AMLEC), and epithelioid AML (EAML) are summarized (Table 1) and the other different imaging features of AMLs including AMLs associated with tuberous sclerosis, haemorrhagic AML, and large AMLs mimicking retroperitoneal liposarcomas are also described. It is important for radiologists to familiarize themselves with the spectrum of AML morphology to be able to establish the correct diagnosis and help clinicians with further treatment planning.

### IMAGING FINDINGS IN ANGIOMYOLIPOMAS

#### Classic AML

On ultrasound, AMLs are typically highly hyperechoic, equal to the echogenicity of renal sinus fat. RCCs and oncocytomas tend to display echogenicity hyperechoic to the renal cortex but less than the echogenicity of renal sinus fat (Figure 1).<sup>4</sup> Despite specific findings that have been described, e.g. posterior shadowing for AMLs, and a hypoechoic rim and internal cysts for RCCs, all echogenic renal lesions should undergo CT for further evaluation.<sup>4</sup> On CT, visible fat density is a hallmark, appearing as an internal hypodense area with attenuation <-10 HU on unenhanced CT (UECT) images.<sup>1</sup> It is important to use thin CT sections (1.5–3 mm) to detect small amounts of fat (Figure 2).<sup>1</sup> Although rare, RCCs may contain macroscopic fat from perinephric fat

Table 1. CT and MRI features of angiomyolipomas

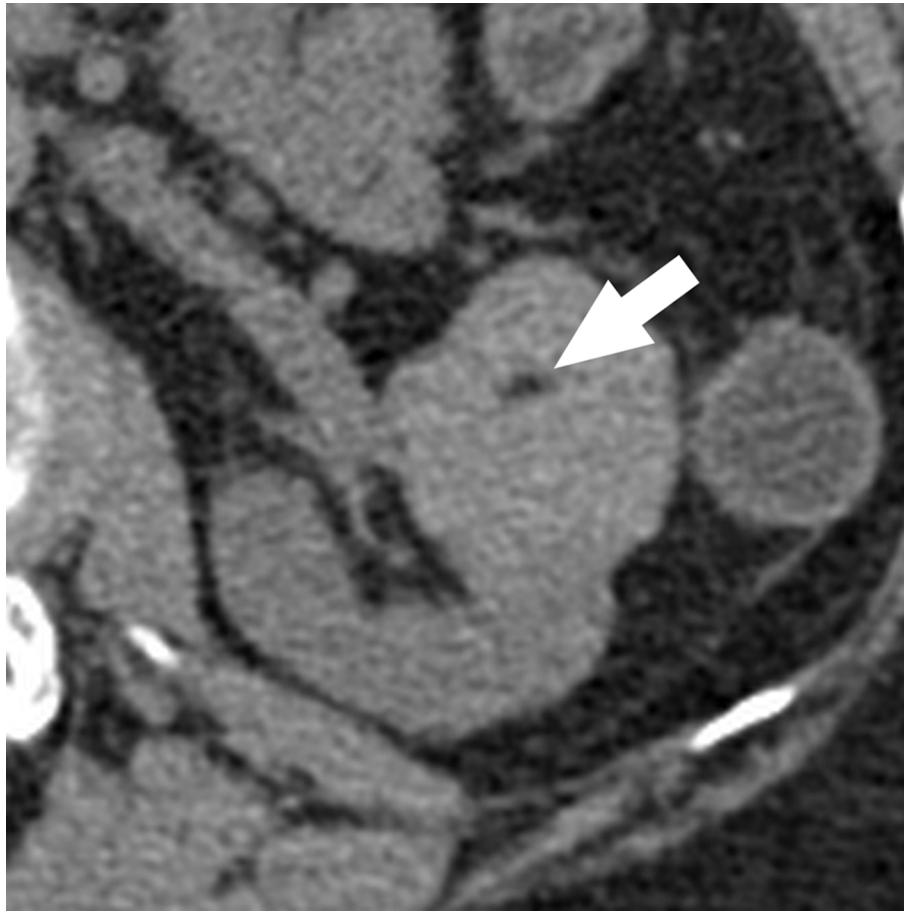
Types of AMLs	CT		MRI	
Classic	UE:	Fat attenuation (<-10 HU)	FS:	Signal drop
		No calcification	CS:	India-ink artefact at macroscopic fat-water interfaces
	CE:	± Intratumoral aneurysm	T <sub>2</sub> W:	Hyperintense area corresponding with signal drop out on fat-suppression image secondary to macroscopic fat
Hyperattenuating fat-poor	UE:	Hyperdense (usually > 45 HU)	FS:	No signal drop
		No fat attenuation	CS:	No signal drop
		No calcification	T <sub>2</sub> W:	Homogeneous hypointense
	CE:	No cystic/Necrotic change		
	CE:	Variable, frequently homogeneous early enhancement with subsequent washout		
Isoattenuating fat-poor	UE:	Isodense (between -10 HU and 45 HU)	FS:	No signal drop
		No fat attenuation	CS:	Signal drop on OP compared with IP
		No calcification	T <sub>2</sub> W:	Hypointense
	CE:	No cystic/necrotic change		
	CE:	Variable, ± gradually progressive enhancement		
AML with epithelial cyst	UE:	Solid part; hyperdense (usually > 45 HU)	FS:	No signal drop
		Cystic part; isodensity	CS:	Solid part; ± signal drop on OP compared with IP.
	CE:	Solid part; ± homogeneous early enhancement with subsequent washout	T <sub>2</sub> W:	Solid part; Hypointense
		Cystic part; ± multiloculated, no enhancement		Cystic part; Bright signal
Epithelioid	UE:	± Fat attenuation	FS:	± Signal drop
		± Calcification	CS:	± Signal drop on OP compared with IP.
		± Internal haemorrhage, Necrosis	T <sub>2</sub> W:	Heterogeneous hypointense
	CE:	Heterogeneous		± Hyperintense from necrosis
		Variable enhancement		
		Presence of vascular invasion		
		Presence of metastasis		

AML, angiomyolipoma; CE, contrast enhanced CT; CS, chemical shift MR image; FS, fat suppression MR image; HU, Hounsfield unit; IP, in phase image; OP, opposed phase image; T<sub>2</sub>W, T<sub>2</sub> weighted MR image; UE, unenhanced CT.

Figure 1. Ultrasound findings of classic angiomyolipoma and renal cell carcinoma. The angiomyolipoma (a, b: white arrows) is highly hyperechoic, equal to the echogenicity of renal sinus fat (asterisk) with posterior shadowing (arrowheads), while the renal cell carcinoma (c: black arrow) is hyperechoic, but less than renal sinus fat (asterisk) and has a hypoechoic rim and internal cysts (open arrows).



Figure 2. Classic angiomyolipoma with a small amount of fat. Axial unenhanced CT image with 1.5 mm sections nicely demonstrates a small amount (arrow) of internal fat attenuation (−48 HU). Note a tiny renal cyst located in the posterior cortex. HU, Hounsfield unit.



engulfment, lipid-producing necrosis, or osseous metaplasia.<sup>5</sup> Atypical oncocytomas with perinephric fat extension can also present as a fat-containing renal mass.<sup>6</sup> Distinguishing AMLs from other fat-containing masses can be aided by other findings.<sup>1,5</sup> AMLs may contain an intratumoral aneurysm, while calcifications suggest RCCs and a central scar is often

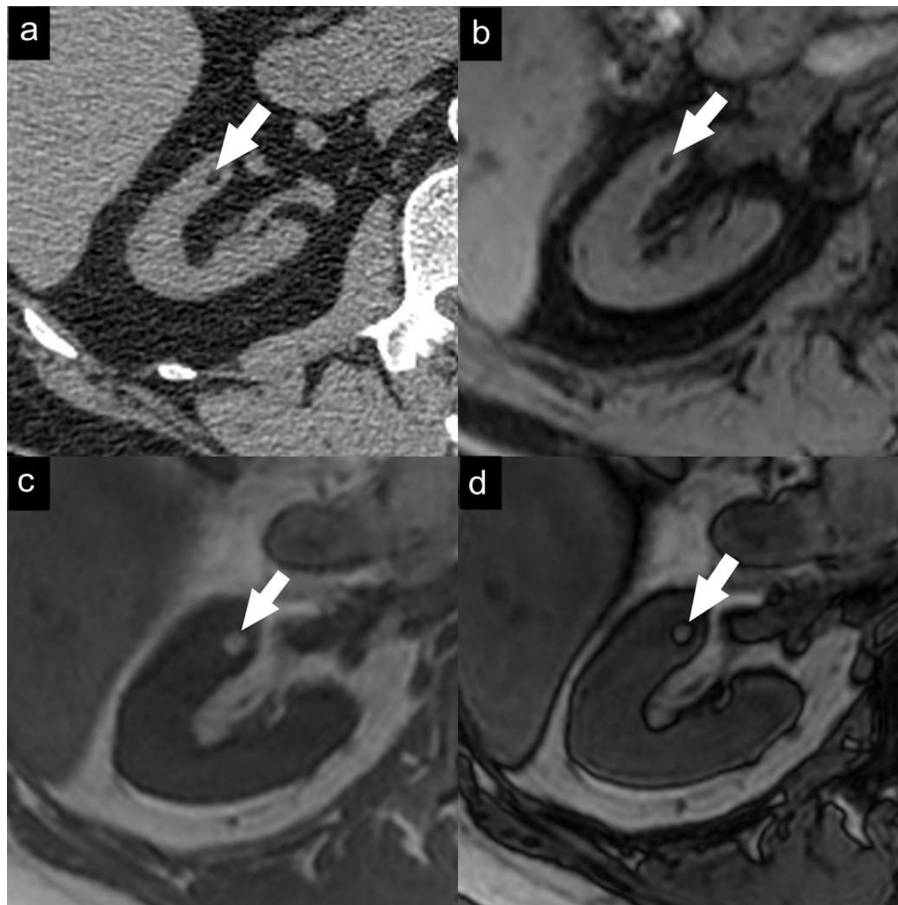
seen in oncocytomas (Table 2).<sup>1,5,6</sup> On MRI, classic AMLs lose signal intensity on fat suppression images (FS-MRI). Chemical shift MRI (CS-MRI) is another sequence that can detect small amounts of fat with signal suppression occurring in voxels containing both fat and water, resulting in an India-ink artefact at macroscopic fat-water interfaces of classic

Table 2. Fat-containing renal masses on CT: imaging clues

	Classic AML	RCC with macroscopic fat	Oncocytoma with perinephric fat extension
Tumour size	Variable	Variable but often large in RCCs with perinephric fat engulfment	Variable
Calcification	− (Rare)	+	±
Intratumoral aneurysm	+	−	−
Cystic/necrotic change	− (Rare)	+	±
Hypervascular mass	+	+	+
Central scar	−	−	+
Vascular invasion	− (Rare)	+	− (Rare)
Distant metastasis	−	+	−

Note: AML, angiomyolipoma; RCC, renal cell carcinoma.

Figure 3. Small classic angiomyolipoma. Axial unenhanced CT image (a) with 1.5 mm sections demonstrates a small fat-containing renal mass (arrow). Axial gradient-echo fat-suppressed  $T_1$  weighted MR image (b) demonstrates a signal drop in the mass due to adipose tissue. Axial  $T_1$  weighted dual-echo in-phase (c) and opposed-phase (d) MR images show a black line between the mass and the renal parenchyma on opposed-phase images (India-ink artefact).



AMLs (Figure 3).<sup>1,3</sup> On contrast-enhanced CT (CECT) and MRI (CE-MRI), a soft tissue part of AMLs can display early enhancement with washout on the nephrographic phase (Figure 4).<sup>7</sup> However, this pattern does not help to distinguish AML from clear-cell RCC (cc-RCC).<sup>7</sup>

#### Fat-poor AML

About 5% of AMLs contain no or minimal fat visible on UECT. Although discriminating fat-poor AMLs from RCCs is difficult,

Figure 4. Classic angiomyolipoma. Axial unenhanced CT image (a) demonstrates a typical fat-containing angiomyolipoma (arrow). Axial  $T_1$  weighted dual-echo in-phase (b) and opposed-phase (c) MR images show an India-ink artefact at the border of the mass and the renal parenchyma on opposed-phase images (double arrows). The mass (arrow) shows early enhancement in the cortico-medullary phase (d) of the axial gradient-echo fat-suppressed  $T_1$  weighted MR image after gadolinium administration. Note two renal cysts adjacent to the AML (asterisks).

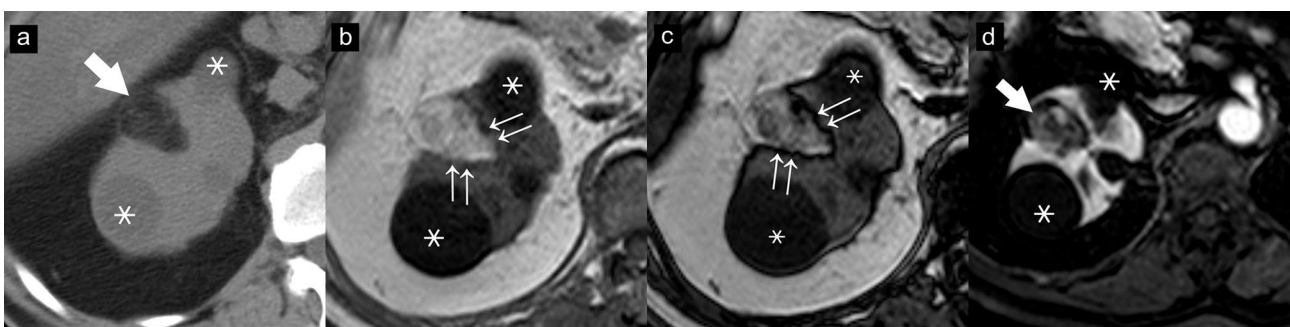


Table 3. Features to differentiate between fat-poor angiomyolipomas vs clear-cell renal cell carcinomas

	Fat-poor AML (hyperattenuating and isoattenuating)	Clear-cell RCC
Tumour heterogeneity	Homogeneous	Heterogeneous
Calcification	Rare	Yes
Cystic/necrotic change	Rare	Yes
Enhancement pattern: early enhancement with subsequent washout	Yes	Yes
Enhancement pattern: gradually progressive enhancement	Possibly	Unlikely
Renal vein invasion	Rare	Yes
Signal drop on OP compared with IP	Possibly (from microscopic fat)	Possibly (from intracytoplasmic fat)
T2WI	Hypointense	Hyperintense
Co-existing classic AMLs	Common	Rare
Syndromic association	TS	VHL, Birt-Hogg-Dubé

AML, angiomyolipoma; IP, in phase image; OP, opposed phase image; RCC, renal cell carcinoma; T2WI,  $T_2$  weighted MR image; TS, tuberous sclerosis; VHL, Von Hippel-Lindau syndrome.

some features on CT and MRI may be useful for diagnosis (Table 3).<sup>7</sup>

#### Hyperattenuating (fat-poor) AML

On CT, about 60% of fat poor AMLs demonstrate hyperattenuation on UECT (>45 HU)<sup>1,3</sup> and homogenous early enhancement with washout on the subsequent phase from their majority of smooth muscles and vessels components.<sup>1,3</sup> Although RCCs can

demonstrate hyperattenuation on UECT, none of them has been reported to be isoechoic on ultrasound, unlike AML.<sup>1,5,7</sup> On MRI, AMLs show hypointensity on  $T_2$  weighted imaging (T2WI) and often no signal drop on either FS-MRI or CS-MRI (Figure 5).<sup>5</sup> In general, RCCs show more heterogeneity and hyperintensity on T2WI, except the papillary subtype (p-RCC), which can be T2-hypointense, possibly due to internal haemorrhage.<sup>7</sup> The

Figure 5. Fat-poor angiomyolipoma, hyperattenuating type. Axial unenhanced CT image (a) demonstrates two right renal masses (arrows) with hyperattenuation (51 and 52 HU) and no visible fat density. On MRI, the masses show no signal drop on axial  $T_1$  weighted dual-echo in-phase (b) and opposed-phase (c) images, and show hypointensity on axial  $T_2$  weighted image (d). Axial gradient-echo fat-suppressed  $T_1$  weighted MR images after gadolinium administration show masses with early enhancement on the corticomedullary phase and washout on the nephrographic phase (the percentage change in signal intensity from corticomedullary (e), nephrographic (f) and excretory phases (g) relative to precontrast phase was 203, 174 and 147% for the mass in the posterior cortex, and 213, 171 and 151% for the mass in the anterior cortex, respectively). The mass in the posterior cortex was proven AML by percutaneous biopsy. HU, Hounsfield unit.

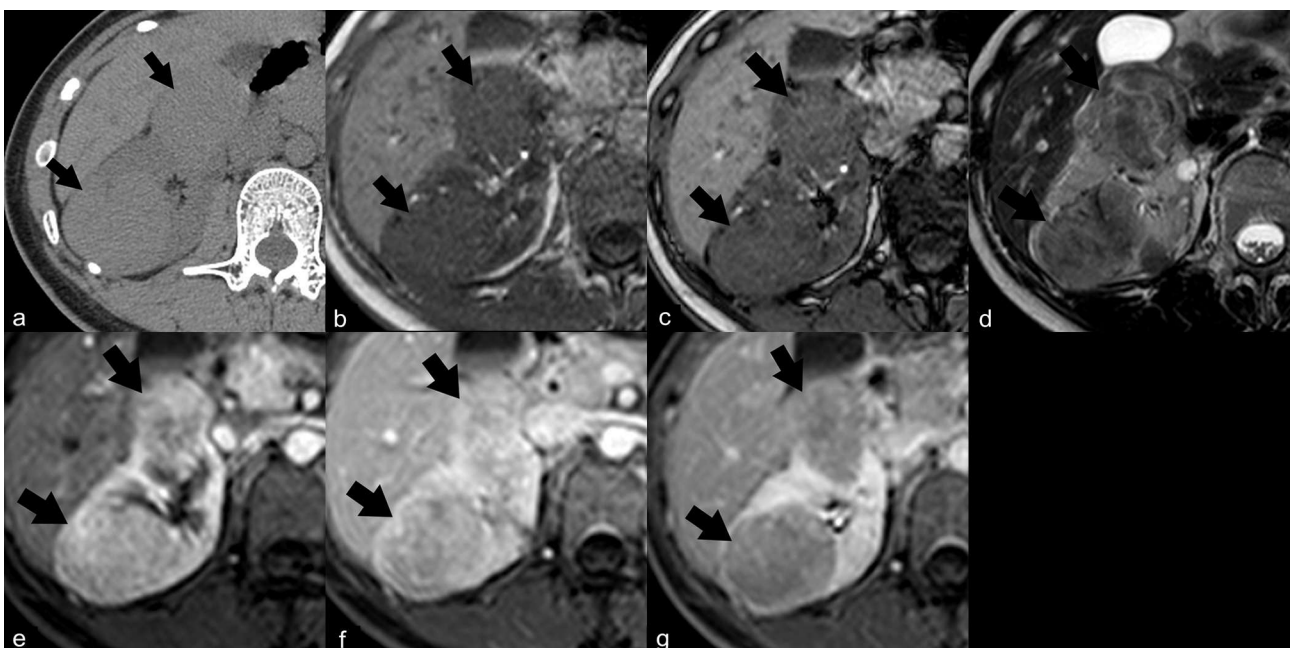
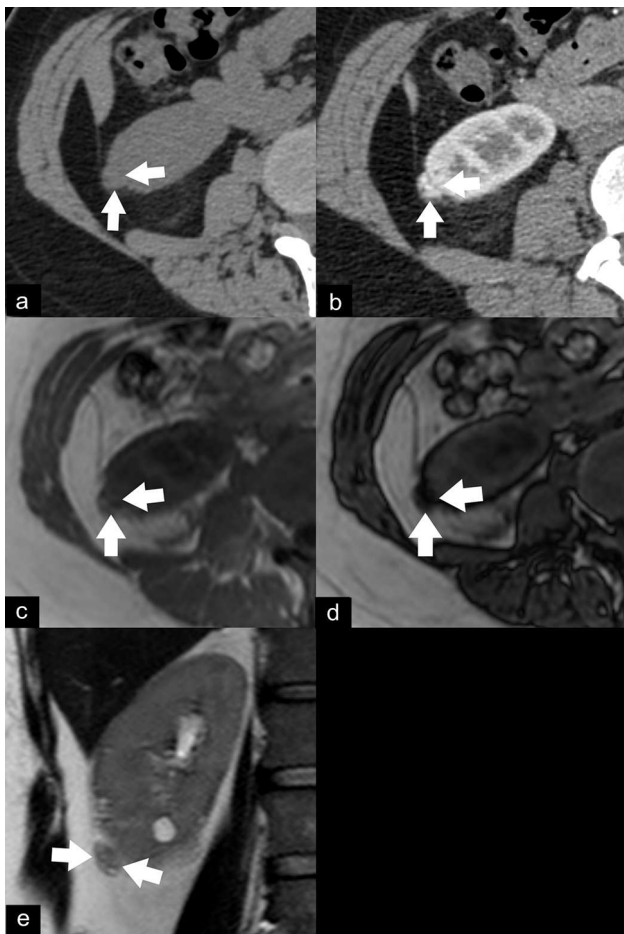


Figure 6. Fat-poor angiomyolipoma, isoattenuating type. Axial unenhanced CT image (a) demonstrates a cortical renal mass (arrows) with isoattenuation (27 HU) and no visible fat density. Axial CECT image demonstrates the mass enhancing in the corticomedullary phase (b). Axial  $T_1$  weighted dual-echo in-phase (c) and opposed-phase (d) images show signal drop within the mass on opposed-phase images. The mass appears slightly hypointense on coronal  $T_2$  weighted image (e). This type of angiomyolipoma is difficult to differentiate from other renal cortical tumours. This mass developed obvious fat components on follow-up 3 year later (not shown). HU, Hounsfield unit.



p-RCCs usually display gradually progressive enhancement, while AMLs demonstrate early enhancement with subsequent washout.<sup>1,5</sup> A T2-hypointense lesion associated with hyperintense signal on  $T_1$  weighted FS-MRI or signal drop on in-phase (IP) compared with opposed-phase (OP) images suggests intratumoral haemorrhage of p-RCC.<sup>3,7</sup>

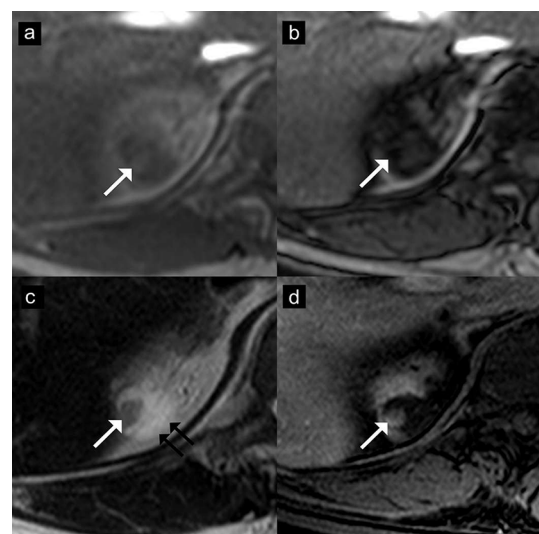
#### *Isoattenuating (fat-poor) AML*

The minority of fat-poor AMLs demonstrate isoattenuation on UECT (-10-+45 HU) and may display gradually progressive enhancement.<sup>1,7</sup> On CS-MRI, isoattenuating AMLs usually show a signal drop on OP compared with IP images from a microscopic fat component (Figure 6).<sup>7</sup> Since RCCs (some cc-RCCs and a few p-RCCs) may contain intracytoplasmic fat resulting in

Figure 7. AMLEC on CT images. Axial unenhanced CT image (a) show a renal mass with peripheral slight hyperattenuation (36 HU) (double arrows). Axial (b) and coronal (c) contrast-enhanced CT images show a cyst with an enhancing peripheral solid nodule (arrows), concerning as a Bosniak category 4 lesion. A partial nephrectomy was performed. The final diagnosis of AMLEC was proven by histopathology. AMLEC, angiomyolipoma with epithelial cysts; HU, Hounsfield unit.



Figure 8. Angiomyolipoma with epithelial cysts (AMLEC) on MR images. Axial  $T_1$  weighted dual-echo in-phase (a) and opposed-phase (b) images show a mass with peripheral signal drop on opposed-phase image (arrows). This lesion shows hypointensity in the solid portion (arrow) and hyperintensity in the cystic portion (double arrows) on axial  $T_2$  weighted image (c). The solid part also shows homogeneous enhancement (arrow) on the axial contrast-enhanced  $T_1$  weighted image (d). The final diagnosis of AMLEC was proven by histopathology.



chemical shift suppression, the T2-signal intensity characteristic should be further evaluated as cc-RCCs and p-RCCs with signal drop are hyperintense, while AMLs are hypointense.<sup>1,3,7</sup> Both cc-RCCs and AMLs can demonstrate signal loss throughout the lesion.<sup>1,3</sup> Unsurprisingly, differentiating RCCs from isoattenuating AMLs is still problematic. Percutaneous biopsy is an option to confirm this diagnosis.<sup>1,5</sup>

#### AML with epithelial cyst—AMLEC

The cystic variant of AML is rare and has been classified as fat-poor, according to the classification by Jinzaki et al.<sup>1</sup> The findings on ultrasound have not been described.<sup>1,5</sup> On CT, AMLECs appear as cysts with enhancing solid components, resembling Bosniak category 4 lesions and mimicking cystic RCCs (Figure 7).<sup>5</sup> The solid part is usually hyperattenuating on UECT, homogeneously enhancing and hypointense on T2WI, which are diagnostic clues.<sup>1,5</sup> A signal drop on CS-MRI may sometimes occur in this type of AML (Figure 8).<sup>1</sup>

#### EPITHELIOID AML (EAML)

A rare type of AML that has malignant potential, EAML occurs in patients with or without TSC.<sup>8</sup> EAMLs are known to be locally aggressive, potentially recurrent, and metastatic.<sup>1</sup> The imaging findings resemble RCCs, which are generally large masses with heterogeneous enhancement, internal haemorrhage, necrosis, and no gross fat component (Figure 9).<sup>8</sup> Tumours can also invade into the renal vein and inferior vena cava (Figure 10).<sup>5</sup> EAMLs demonstrate isoattenuation or hyperattenuation on UECT and are hypointense on T2WI, with or without a signal drop on CS-MRI (Figure 10).<sup>1</sup>

Figure 9. Epithelioid angiomyolipoma (EAML). Ultrasound (a) demonstrates a large heterogeneous hyperechoic mass in the right kidney (arrows). Axial unenhanced CT image (b) shows a 14 cm renal mass (arrows) with internal calcifications (arrow heads) and no gross fat component. Coronal contrast-enhanced CT image (c) shows the heterogeneous enhancing mass (arrow) in the lower pole of the right kidney which compresses the renal pelvis, causing mild dilatation of the upper pole calyces (double arrows). Renal cell carcinoma was suspected and a radical nephrectomy was performed. The final diagnosis of EAML was proven by histopathology and immunohistochemistry.

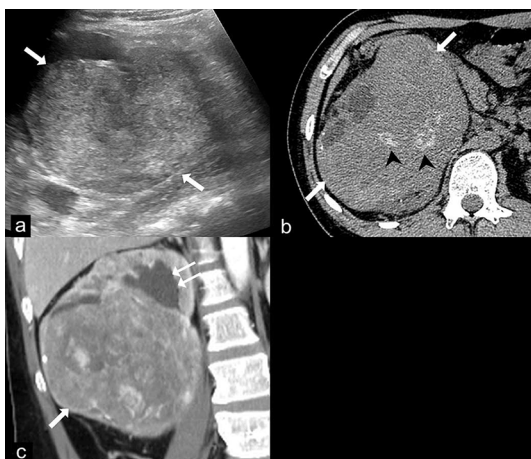
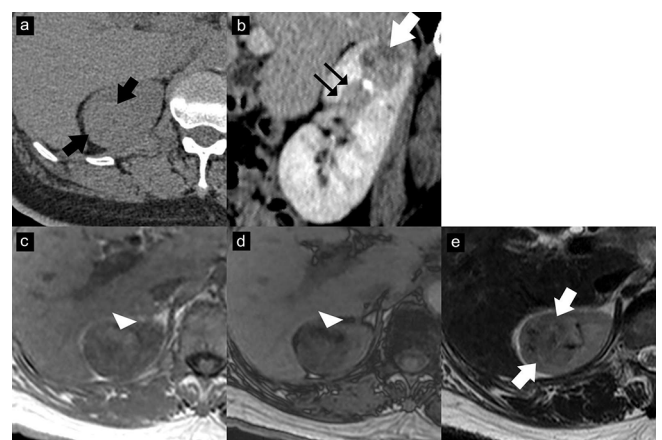


Figure 10. EAML with segmental renal vein invasion. Axial unenhanced CT image (a) shows an isoattenuating renal mass (37 HU) without calcification or gross fat component (arrows). Contrast-enhanced CT image with sagittal multiplanar reconstruction in the nephrographic phase (b) shows a heterogeneously enhancing mass (arrow) in the upper pole with extension into a segmental renal vein (double arrows). Axial T<sub>1</sub> weighted dual-echo in-phase (c) and opposed-phase (d) images show signal drop in the anterior part of the mass on the opposed-phase image, representing intracytoplasmic lipid (arrowhead). This lesion shows iso-to-hypointensity (arrows) on the axial T<sub>2</sub> weighted image (e). The mass was resected due to segmental renal vein invasion. The final diagnosis of EAML was proven by histopathology and immunohistochemistry. EAML, epithelioid angiomyolipoma; HU, Hounsfield unit



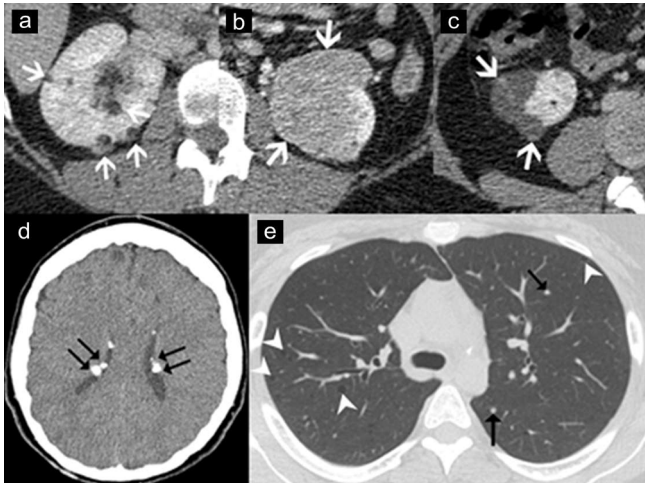
#### AML associated with tuberous sclerosis

Renal AMLs occur in the TSC patients as high as 90%, and are commonly multiple, bilateral, and often symptomatic due to spontaneous bleeding.<sup>2</sup> AMLs in TSC patients have a faster growth rate and are more likely to be fat-poor types such as EAML and AMLEC (Figure 11).<sup>1,8</sup>

#### HAEMORRHAGIC AML

Haemorrhage, a complication of AML, causes increased internal density within the mass, obscuring the underlying fat.<sup>5</sup> AMLs sometimes produce massive retroperitoneal bleeding.<sup>5</sup> The only way to differentiate AMLs from other haemorrhagic renal lesions is the presence of intratumoral fat on the previous or follow-up imaging studies (Figure 12).<sup>5</sup> Risks of haemorrhage relate to AML  $\geq 4$  cm or intralésional aneurysms  $>5$  mm, these being traditional criteria for intervention.<sup>9</sup> Currently, embolization is the first-line management in cases of active bleeding with haemodynamic instability, and also an option when surgery is otherwise not possible.<sup>9</sup> Compared with surgery, embolization results in less renal parenchymal volume loss and a shorter hospital stay.<sup>9</sup> However, it carries a 10–20% higher risk of tumour regrowth or re-bleeding, and eventually, repeated embolisation is required.<sup>9</sup> In TSC patients, nephron-sparing surgery is a more favourable option due to the lower recurrence rate.<sup>9</sup> The decision to treat asymptomatic patients should be based

Figure 11. Angiomyolipoma (AML) associated with tuberous sclerosis. Axial contrast-enhanced CT images of a 40 year-old-woman with tuberous sclerosis, demonstrating multiple typical AMLs (a: arrows), a fat-poor AML (b: arrows), and angiomyolipomas with epithelial cysts (c: arrows). Axial CT image of brain (d) in the same patient shows multiple calcified subependymal tubers (double arrows). Axial CT image of the chest (e) demonstrates multiple well-defined lung cysts (arrowheads) and multiple tiny nodules (arrows), which are consistent with lymphangiomyomatosis and multifocal micronodular pneumocyte hyperplasia, respectively.

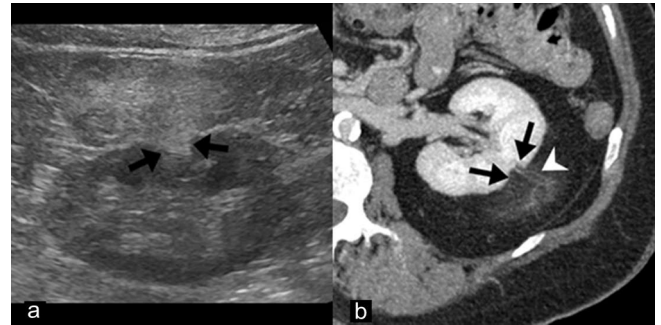


on multiple factors and observation may be a good option in the selected asymptomatic cases despite no currently established consensus guidelines.<sup>9</sup>

#### AML mimics retroperitoneal liposarcoma

Differentiation of large AMLs from retroperitoneal liposarcomas or other retroperitoneal fat-containing tumours can be achieved by demonstrating signs that indicate renal origin, such as the claw sign, described as renal parenchyma draping

around the mass, and feeding vessels supplied from the kidneys (Figure 13).<sup>10</sup>



around the mass, and feeding vessels supplied from the kidneys (Figure 13).<sup>10</sup>

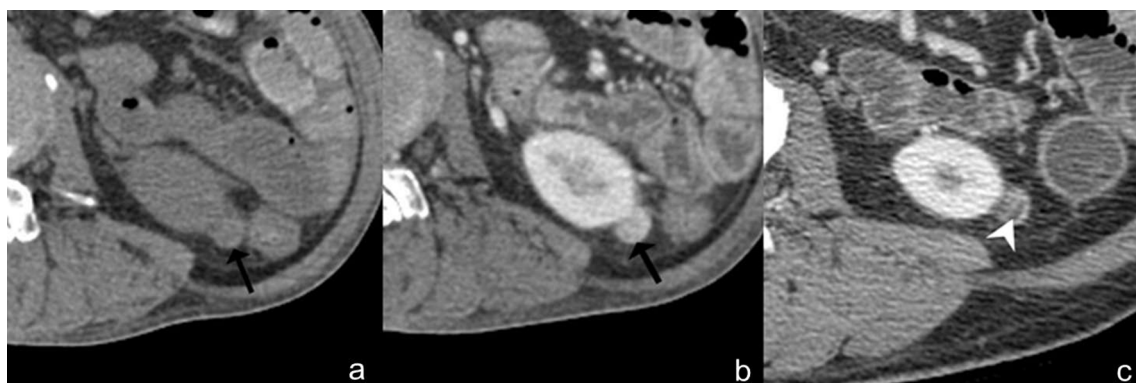
#### SUMMARY

In addition to typical fat-containing renal lesions, AMLs may have various appearances from cystic to solid, which overlap with other renal tumours. Radiologists should look for the imaging features that point towards AMLs.

#### TEACHING POINTS

- A visible fat density on UECT is a hallmark of renal AMLs.
- Hyperattenuating fat-poor AMLs usually demonstrate hyperattenuation on UECT and homogeneous  $T_2$ -hypointensity, while RCCs typically show more heterogeneous attenuation and are  $T_2$ -hyperintense.
- The solid part of AMLEC may demonstrate hyperattenuation on UECT and hypointensity on T2WI, similar to hyperattenuating AMLs.
- EAMLs have a malignant potential and resemble RCCs.

Figure 12. Angiomyolipoma with internal haemorrhage. Axial unenhanced (a) and contrast-enhanced CT (b) images show an isoattenuating renal mass (28 HU) with homogeneous enhancement, no calcification or fat component (arrow). Based on these findings, the differential diagnosis includes renal cell carcinoma, oncocytoma or isoattenuating angiomyolipoma. However, typical angiomyolipoma with internal haemorrhage can be diagnosed due to the presence of intratumoral fat (arrowhead) on the previous image (c). HU, Hounsfield unit.





- Haemorrhage in AMLs may obscure fat. Correlation with prior or follow-up imaging can confirm the diagnosis.
- Large AMLs can be distinguished from retroperitoneal liposarcomas by detecting signs indicating renal origin.

## REFERENCES

1. Jinzaki M, Silverman SG, Akita H, Nagashima Y, Mikami S, Oya M. Renal angiomyolipoma: a radiological classification and update on recent developments in diagnosis and management. *Abdom Imaging* 2014; **39**: 588–604. doi: <https://doi.org/10.1007/s00261-014-0083-3>
2. Kapoor A, Girard L, Lattouf JB, Pei Y, Rendon R, Card P, et al. Evolving strategies in the treatment of tuberous sclerosis complex-associated angiomyolipomas (TSC-AML). *Urology* 2016; **89**: 19–26. doi: <https://doi.org/10.1016/j.urology.2015.12.009>
3. Song S, Park BK, Park JJ. New radiologic classification of renal angiomyolipomas. *Eur J Radiol* 2016; **85**: 1835–42. doi: <https://doi.org/10.1016/j.ejrad.2016.08.012>
4. Farrelly C, Delaney H, McDermott R, Malone D. Do all non-calcified echogenic renal lesions found on ultrasound need further evaluation with CT? *Abdom Imaging* 2008; **33**: 44–7. doi: <https://doi.org/10.1007/s00261-007-9306-1>
5. Schieda N, Kielar AZ, Al Dandan O, McInnes MD, Flood TA. Ten uncommon and unusual variants of renal angiomyolipoma (AML): radiologic-pathologic correlation. *Clin Radiol* 2015; **70**: 206–20. doi: <https://doi.org/10.1016/j.crad.2014.10.001>
6. Ishigami K, Jones AR, Dahmouh L, Leite LV, Pakalniskis MG, Barloon TJ. Imaging spectrum of renal oncocytomas: a pictorial review with pathologic correlation. *Insights Imaging* 2015; **6**: 53–64. doi: <https://doi.org/10.1007/s13244-014-0373-x>
7. Lim RS, Flood TA, McInnes MDF, Lavallee LT, Schieda N. Renal angiomyolipoma without visible fat: can we make the diagnosis using CT and MRI? *Eur Radiol* 2018; **28**. doi: <https://doi.org/10.1007/s00330-017-4988-4>
8. Tsukada J, Jinzaki M, Yao M, Nagashima Y, Mikami S, Yashiro H, et al. Epithelioid angiomyolipoma of the kidney: radiological imaging. *Int J Urol* 2013; **20**: 1105–11. doi: <https://doi.org/10.1111/iju.12117>
9. Flum AS, Hamoui N, Said MA, Yang XJ, Casalino DD, McGuire BB, et al. Update on the diagnosis and management of renal angiomyolipoma. *J Urol* 2016; **195**(4 Pt 1): 834–46. doi: <https://doi.org/10.1016/j.juro.2015.07.126>
10. Israel GM, Bosniak MA, Slywotzky CM, Rosen RJ. CT differentiation of large exophytic renal angiomyolipomas and perirenal liposarcomas. *AJR Am J Roentgenol* 2002; **179**: 769–73. doi: <https://doi.org/10.2214/ajr.179.3.1790769>